



Adaptive Optics for Confocal Microscopy using the Optimization of Molecular Brightness

Bojan Mavkov

► To cite this version:

Bojan Mavkov. Adaptive Optics for Confocal Microscopy using the Optimization of Molecular Brightness. [Intern report] Joseph Fourier. Université Joseph Fourier (Grenoble 1) (UJF), Grenoble, FRA. 2013. hal-03751359

HAL Id: hal-03751359

<https://hal.science/hal-03751359>

Submitted on 14 Aug 2022

HAL is a multi-disciplinary open access archive for the deposit and dissemination of scientific research documents, whether they are published or not. The documents may come from teaching and research institutions in France or abroad, or from public or private research centers.

L'archive ouverte pluridisciplinaire **HAL**, est destinée au dépôt et à la diffusion de documents scientifiques de niveau recherche, publiés ou non, émanant des établissements d'enseignement et de recherche français ou étrangers, des laboratoires publics ou privés.



gipsa-lab



UNIVERSITE JOSEPH FOURIER

MASTER 2, INTERNSHIP REPORT

Adaptive Optics for Confocal Microscopy using the Optimization of Molecular Brightness

Author:

MAVKOV Bojan

Supervisors:

Dr.VODA Alina (Gipsa-lab)

Dr.DELON Antoine (LIPhy)

Dr.LEROUX Charles-Edouard(LIPhy)

June 17, 2013

Contents

1	Description of the system	2
1.1	Introduction	2
1.2	Experimental setup and materials	3
1.3	Modeling	3
1.4	Estimation of CRM	6
1.5	Creating the simulation data	7
1.6	Strategy for the aberration correction	7
2	Description of the methods	10
2.1	Non-gradient based methods	10
2.1.1	Hill-climbing algorithm	10
2.1.2	Multivariable interpolation	11
2.1.3	N-points single mode interpolation	11
2.2	Gradient based methods	12
2.2.1	Gauss-Newton algorithm	12
2.2.2	Levenberg - Marquardt algorithm	13
2.2.3	Single mode correction	14
3	Implementation and results	16
3.1	Non-gradient based methods implementation results	16
3.1.1	Results from the testing on the real system	16
3.2	3N-algorithm for optimization	17
3.2.1	Comparison of the two algorithms	17
3.2.2	Multivariable interpolation results	17
3.3	Gradient based method implementation	18
3.4	Levenberg- Marquardt algorithm	18
3.5	Optimization with fminunc and fminsearch	19
3.6	Implementation of the model-based methods on the real systems data	21
4	Conclusions and future improvements	24
5	The First Appendix, Zernike polynomials	27
6	The Second Appendix, Pseudocode for the HC algorithm	30
7	The Third Appendix, Estimation of N	31
8	The Fourt Appendix, Inversion with SVD	32

Abstract

The main goal of this work is to develop and test several methods for aberration correction with using adaptive optics in Florescence Correlation Spectroscopy. Here the quantification of the influence of the aberrations in single photon FCS is used for the correction metric of the adaptive optics. The main idea of this thesis was based on the previous work [2] of C.E.Leroux, I.Wang, J.Derouard and A.Delon that suggest that the count rate per molecule,CRM(or molecular brightness) can be used as an optimization metric when applying Adaptive Optics to biological media.Morover, the first simulations of such a system have been initiated in the work [1] of Tudor-Bogdan Airimitoie. Testing of the methods is performed first on the generated simulation data and after performed on the real system.

List of abbreviations

- λ laser's wavelength
- CRM Count rate per molecule
- N Mean number of molecules
- CR Count rate
- n Number of photons
- a_i^{ab} Aberration of Z_i , Zernike mode i
- a_i^c Corrected aberration of Z_i , Zernike mode i
- $\Phi(r, \theta)$ Input aberration
- $\Psi(r, \theta)$ Corrected aberration
- J_r Jacobean
- σ_{wf}^2 Root Mean Square(RMS) of the aberrations
- β Unknown parameters for identification
- S, S_1, S_2, S_3 Cost functions used for optimization
- y_i Measurement in point i
- r_i Measurement error in point i

Chapter 1

Description of the system

1.1 Introduction

Recent breakthroughs in scientific instrumentation significantly have improved the resolution of (scanning) optical microscopy and related imaging systems. One emerging technology is Adaptive Optics (AO). Based on micromechanical deformable mirrors, AO enables to compensate for aberrations in the imaging system and to improve overall resolution.

Here mechatronic system design and modern control engineering also indicate huge innovation potential to enhance system performance in terms of speed and resolution.

This research in mechatronics of imaging systems will address the development of novel optimization methods for wave front correction, as well as improved operation of optical microscopes, particularly scanning of confocal microscopes for bio-medical research. The work is based on the work on the research in the interdisciplinary laboratory for physics LIPhy, UJF Grenoble.

The control of the shape of the adaptive mirror in adaptive optics is performed to correct the aberrations from the measurement. In an imaging system, aberrations occur when light from one point of an object does not converge into a single point after transmission through the system. Deformable mirrors (DM) are mirrors whose surface can be deformed, in order to achieve wavefront control and correction of optical aberrations.

The sample in the microscope is illuminated by the beam from the laser. The light goes to the sample and gets out aberrated. This signal goes to the detector of fluorescence that is used for measurement of photons. In the system build in LIPhy, the estimation of the aberration should be done by the detector of fluorescence, by the number of measured photons in a period of time. In this case the wavefront sensor is not used for the detection of the aberration, because of lack of optical sectioning capability. The main research is based on finding the appropriate methods and their implementation for the wave front sensor-less adaptive optics problem based on the research and equations developed in LIPhy.

This work will present several phases in adaptive optics :

- Defining the system and the metrics, modeling the aberrations and the strategies for the controlling the shape of the adaptive optics.
- Describing the methods that are used for the controlling the shape of the deformable mirror.
- Implementation, testing and comparing the performances of the methods performed on the AO

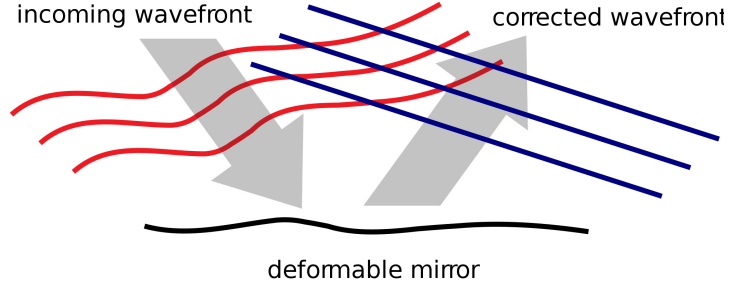


Figure 1.1: Adaptive optics systems use a deformable mirror to correct wavefront distortions

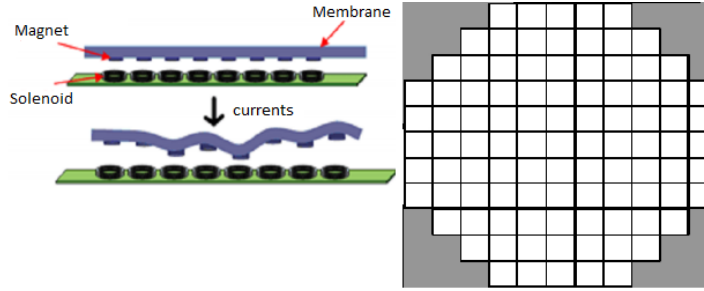


Figure 1.2: 97 element ALPAO Deformable Mirror,(left) Structure of the mirror,(right) Actuator geometry of the deformable mirror

1.2 Experimental setup and materials

The optical system of our experiment is based on an Olympus X71 platform using a C-Apochromat 63X/1.2 W Korr water objective manufactured by Zeiss and a fluorescence cube with a dichroic mirror and an emission filter. The system also consists of Shack-Hartmann Wavefront Sensor(SHWFS) for calibration of the deformable mirror. The using of SHWFS for aberration measurements is not possible in this case because of lack of optical sectioning capability. The laser beam at 633 nm (HeNe, from Thorlabs) has an uniform intensity profile in the pupil plane of the objective, which is required to have an uniform signal to noise ratio on the Shack-HartmannWavefront Sensor (SHWFS) when performing the calibration of the DM. For the correction of the aberrations, 97 actuators Hi-speed deformable mirror(manufactured by ALPAO) is used. The control of the shape of the mirror is made by sending separately control signal to each actuator of the mirror(Fig. 1.2). The used DM has ability to generate with good precision Zernike aberrations of large amplitudes. The system is presented in Fig. 1.3.

1.3 Modeling

The optical aberrations depend on the optical alignment, reflective index, observation depth and other factors. This means, that if we want to perform correction of the aberrations , we need to perform the correction in similar or exact conditions like the experiment that we are interested in. There are several metrics that are important when the Florescence Correlation Spectroscopy is performed. The mean number of molecules

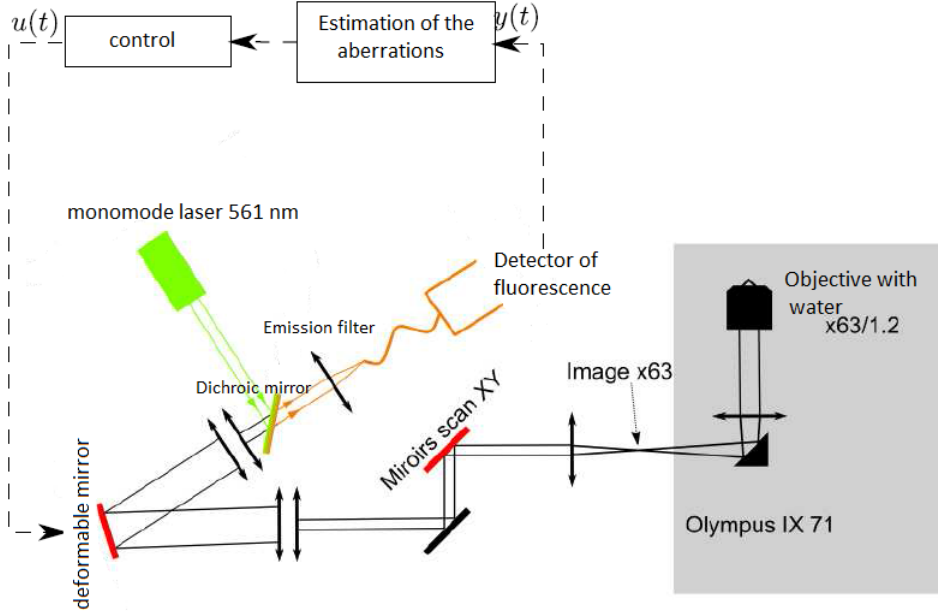


Figure 1.3: The optical system with the control

in the FCS observation volume, N is one of this measured metrics. There are several other parameters connected to N , the molecular brightness, defined as the Count Rate per Molecule, CRM, and the total Count Rate, CR. The measurements of this metrics is directly connected with the intensity of the aberrations of the observed experimental sample. The main idea of performing the aberration correction in this system is to use the measurement of one of this metrics to measure the intensity of the aberrations on it. For this aim, the most important thing is to provide the mathematical relations that connect this metrics with the amount of the aberrations in the measured sample. The parameter CRM can be well approximated with the following expression:

$$\overline{CRM}^{ab} = \overline{CRM}^{opt} \cdot e^{-2(\frac{2\pi\sigma_{wf}}{\lambda})^2} \quad (1.1)$$

where the σ is presented by:

$$\sigma_{wf}^2 = \sum_i (a_i^{ab} - a_i^c)^2 \quad (1.2)$$

σ_{wf} presents the Root Mean Square(RMS) of the aberrations (of both illumination and detection beam) and λ is the mean value of the excitation and fluorescence wavelengths. The value of wavelengths is $\lambda = 580nm$ in this case. In practice, the amplitudes, a_i^{ab} of Zernike aberrations introduced by the sample can be estimated, by assuming that the aberrations are perfectly corrected by the DM. For each Zernike mode i , the notation a_i is for the amplitude of that mode i . The aberration of the input can be presented as a series of Zernike polynomials, each denotes as $Z_i(r, \theta)$:

$$\Phi(r, \theta) = \sum_i a_i^{ab} Z_i(r, \theta) \quad (1.3)$$

and the corrected aberrations from the deformable mirror can be presented as a similar series, but parameterized by a_i^c :

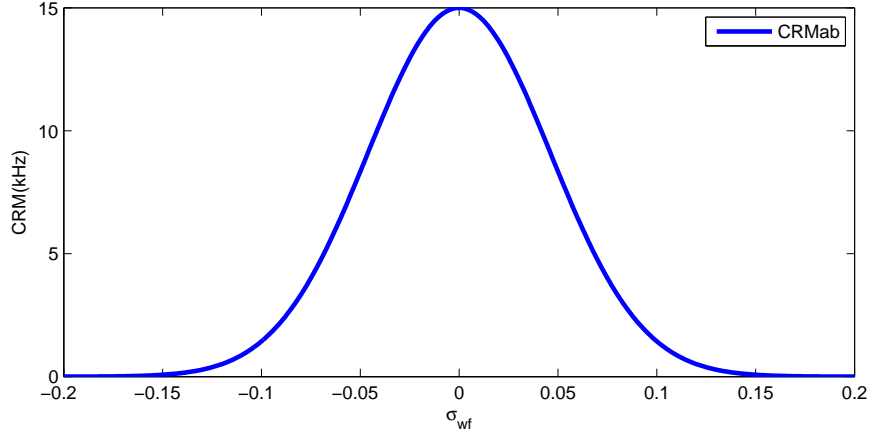


Figure 1.4: Plot of CRM in function of σ_{wf}

$$\Psi(r, \theta) = \sum_i a_i^c Z_i(r, \theta) \quad (1.4)$$

The other metric that can be presented in relation to the aberrations in the system is the mean number of molecules, N measurement. The equation is obtained by fitting a curve on the measured data (presented on Fig. 1.5). The equation for calculating N is different for each single mode that is examined. In our case the relation for the modes a_{13} and a_{25} is presented:

$$\bar{N}^{ab} = \bar{N}^{opt}(1 + \alpha\sigma_{wf}^\beta) \quad (1.5)$$

where:

- for a_{13} : $\alpha = 321$ and $\beta = 2.140$
- for a_{25} : $\alpha = 2847$ and $\beta = 2.89$

The measured number of photons in the experiment can be presented according to the CRM and N as:

$$\bar{n}^{ab} = \overline{CRM}^{ab} \cdot \bar{N}^{ab} \cdot \delta t, \quad (1.6)$$

where δt presents the sampling time in our system. In this system its value is $\delta t = 1\mu sec$

The total Count Rate, CR can be calculated as:

$$\overline{CR}^{ab} = \frac{\bar{n}^{ab}}{\delta t} \quad (1.7)$$

and the relation between CRM , CR and N can be presented as:

$$\overline{CRM}^{ab} = \frac{\overline{CR}^{ab}}{\bar{N}^{ab}} \quad (1.8)$$

We can notice that the CRM in our system is a good metric to be used for the identification and the correction of the aberrations. With the Equation 1.1 the relation between the aberrations and the CRM is well presented for all of the modes and it can be used for the identification of the aberrations. In this system the values of the parameters vary in the ranges:

- CRM in range of $1 \div 30kHz$
- N in range of $1 \div 150$ molecules.

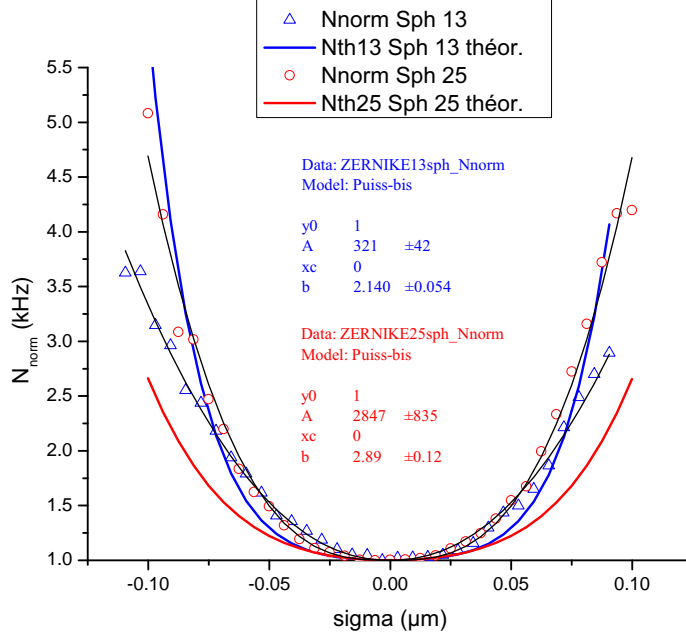


Figure 1.5: measurements and estimation of N in function of $\sigma_w f$

1.4 Estimation of CRM

The detector of fluorescence that is used in our system gives the number of the measured photons as the output of its measurements. The main parameter that is going to be used for the optimization of the deformable mirror is the *CRM*. This means that we need to use the estimated number on photons and with the knowledge of the sampling time of the system δt we should estimate the *CRM* that will be used for the aberration correction.

The estimated *CR* is calculated according to:

$$\widehat{CR} = \frac{\bar{n}}{\delta t} \quad (1.9)$$

The number of molecules, N can be estimate using this two formulas:

$$\hat{N} = \frac{\bar{n}^2}{n(t)n(t + \delta t) - \bar{n}^2} \quad (1.10)$$

$$\hat{N} = \frac{\bar{n}^2}{var(n) - \bar{n}} \quad (1.11)$$

After testing these equations on the simulation, the second equation(1.11) proved to be more accurate for estimation of N . The results of the simulation are presented in the Third Appendix.

Using the estimated values of the *CR* and N , the estimated *CRM* can be calculated as:

$$\widehat{CRM} = \frac{\widehat{CR}}{\hat{N}} \quad (1.12)$$

1.5 Creating the simulation data

Before we test the proposed methods on the real system, testing should be performed on data obtained by simulation of the system. On the simulation data the aberration is presented by using the equations: 1.1 and 1.5. The measurement of the photons is simulated by using 1.6. To present the real system and the measurement noise that is presented, noise is added using the Poisson distribution. The density probability function is calculated by:

$$P(k) = P(X = k) = \frac{\lambda^k e^{-\lambda}}{k!} \quad (1.13)$$

the mean value and the variance:

$$\hat{X} = \lambda \quad (1.14)$$

$$var(X) = \lambda \quad (1.15)$$

The measurement noise that is added is 2000 photons per second.

After the measured number of photons are simulated, CRM is estimated using the equations: 1.9, 1.11 and 1.12.

1.6 Strategy for the aberration correction

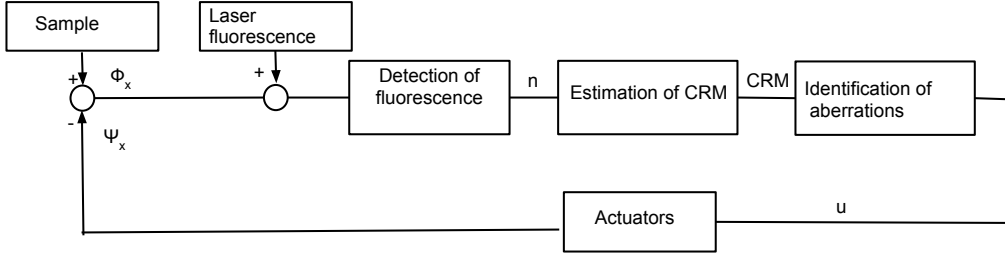


Figure 1.6: Block representation of the system

There are several aspects that are important when the optimization and the identification methods need to be applied. The biggest obstacle that should be avoided at the beginning of the optimization is the coupling between the modes. When the measurements are performed on the real system, there is coupling between some of the modes that is not modeled with the theoretical model of the system. There are a lot of publications concerning the control of the shape of deformable mirror applied in large telescopes and in microscopes. All of this works have different approaches according to the particularities of the systems where they are implied. When it comes to the choice of the algorithms, in our case there are some of the particularities that we need to keep on mind:

- There are coupling between the modes. The coupling in the equations for the system are not modeled. This means that, at the beginning some robust, non-gradient based method should be applied for the optimization.
- Before the optimization is performed, using the SHWFS sensor, the shape of the mirror can be calibrated for each Zernike mode separately. The optimization in this system can be performed by optimizing the amplitude for each Zernike mode

instead of performing control of the shape by sending voltages to every actuator in the mirror separately. This approach will reduce the calculation time and have better convergence speed. Also, this method eliminates the local optimum problem that can be present if the optimization is performed on the voltage of the actuators separately.

- In this case, the measurements are performed on real biological materials and because of this, the measurement signal is with low intensity. This means that, the measurement time is relatively longer comparing to the other similar works on adaptive optics and the methods that are implied should be fast, with low number of iterations required.
- We have some *a priori* knowledge about the modes that are most influential for the aberration in our system and also we know the pairs of modes that are coupled. This knowledge can be used for the optimization methods to correct the modes with the highest impact in order to reduce the optimization time. In our system the modes a_{13} and a_{25} are coupled modes and they are the ones that are corrected first. Other modes that should be corrected are: a_4 (defocus), a_6 (astigmatism), a_7 and a_8 (coma), a_9 and a_{10} (trefoil).
- After most of the dominant modes are corrected, coupling in the system can be neglected and we can use the developed model of the system as correct. When the coupling is neglected, relation between the measured CRM and the aberrations in the system(σ_{wf}) is good modeled. This formula can be used for the estimation of the aberrations in our measurements. Gradient based methods can be developed for the optimization based on this relations.

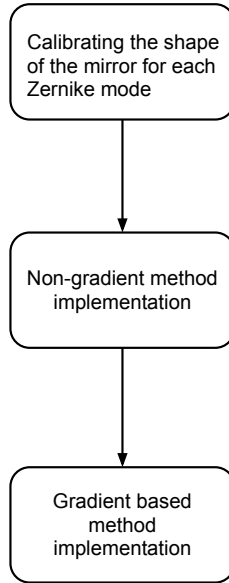


Figure 1.7: Execution order of the implied methods

The correction of the aberrations consist of three main phases. First, before the optimization is performed, the shape of the mirror is calibrated for each Zernike mode.

After the shapes are obtained, the optimization can be performed. The first methods that are going to be performed are the non-gradient methods. After the optimal solution is found by this methods, the gradient based methods are implemented for the identification of the aberrations.

Chapter 2

Description of the methods

2.1 Non-gradient based methods

In order to avoid the non-modeled coupling between the modes, first we implemented the Non-gradient based methods for optimization. Different optimization methods were performed. Because the measurement time for one iteration in our system is relatively long, the main goal for choosing the appropriate algorithm was to find the algorithm that can be executed in small number of steps and that should be robust to the coupling and the noise that it present in the measurements. For this aim this main algorithms were performed:

- Hill-climbing algorithm
- 3N-interpolation algorithm
- Combination of multivariable interpolation and single mode interpolation

2.1.1 Hill-climbing algorithm

Hill-climbing algorithm is optimization technique that tries to find the solution using a local search. This method starts from some initial point and tries to find the optimal solution by moving around that point. This method is excellent for finding optimal solution by optimizing convex surfaces, because in this functions the global maximum can be found. The equation that presents CRM in function of the amplitude of the Zernike modes has convex shape, this means that this method is adequate to be implemented for finding the optimal solution in our system.

Similar Hill-climbing(for discrete systems) approach was used in the work [4] where it was performed on every actuator separately and it took around 300 iterations for the optimization. Later, the same method was used performed on optimization of Zernike modes and was presented on [5]. The optimization performed on Zernike modes was faster and more accurate because the global maximum is easier to be obtained. When the optimization is performed on the Zernike modes the function is convex and there is only one global maximum. This optimization will be performed only on several modes separately. First, the optimization is performed once for every mode separately and after that it is repeated several times. During the testing some of the parameters that should be defined in the algorithm like the *Step size* and the *acceleration* should be defined and tested on the simulation data and after on the real system. The value of this parameters is very important for the optimization performances. The *acceleration* has initial, fixed value and the *Stepsize* changes its initial value, according to the convergence

or divergence from the optimal point.

In our case the Continuous Space Hill Climbing Algorithm that is different to the discrete one used in previous works [5]. The method is implemented for 4 seconds measurement and one iteration for single mode needs 5 measurement points. This optimization will be performed only on the most dominant modes. First, the optimization is performed once for every mode separately and after that, it is repeated several times in cycles in the same order until the optimization reaches some steady state. The pseudo-code for the Continuous Space Hill Climbing Algorithm is presented on the second Appendix.

2.1.2 Multivariable interpolation

Because some of the most dominant modes a_{13} and a_{25} are coupled in reality and the optimization on this mode will be better if it is performed on the both modes at the same time. For this aim, multivariable interpolation can be performed on this modes and in all the modes that are considered as coupled. With the multivariable interpolation, the representation of CRM can be presented as function of two variables that can take in account the relation of the measured metric in function of the two coupled modes.

To perform a multivariable interpolation, $N \times N$ measurements should be performed on the both modes, where N is the number of measurements per one mode. The measurements are taken by changing the values of a_{13}^c and a_{25}^c in this case that are in range of $\pm 0.05\mu m$. If we take $N = 5$ for better precision of the optimization, the total number of measurement per one iteration is $5^2 = 25$ measurements.

Because the system runs on MATLAB based platform, the build-in MATLAB functions can be used for the Multivariable interpolation implementation. The "interp" function is used for the multivariable interpolation. There are several methods that can be used for interpolation by using this function:

- Nearest neighbor interpolation
- 'linear'- Linear interpolation (default)
- 'spline'- Cubic spline interpolation
- 'cubic' -Cubic interpolation, as long as data is uniformly-spaced. Otherwise, this method is the same as 'spline'.

After the multivariable interpolation is done for the coupled modes, the maximum of the interpolated function can be found. The points of a_{13} and a_{25} , where the interpolated function receives its maximum are taken as the optimal point, and their value is sent as the control signal for the deformable mirror. If the measurements are on the boundaries of the measured aberrations for some mode on the interpolated curve, the measurement point for this mode are shifted for the next optimization iteration.

2.1.3 N-points single mode interpolation

The optimization process can be done on every mode separately by taking measurements for each different mode. By changing the a^c for each mode in the range of $\pm 0.05\mu m$ the points for the measurements for CRM are obtained. After the measurements are taken the interpolation curve is obtained and the maximum point is calculated in the interpolated curve for the single mode. The point for a^c where the maximum is estimated is taken as the identified value for the aberration intensity for that particular mode. The Lagrangian interpolation performed in three point $a^c = -0.05, 0, 0.05\mu m$ can be noted as 3N algorithm for optimization.

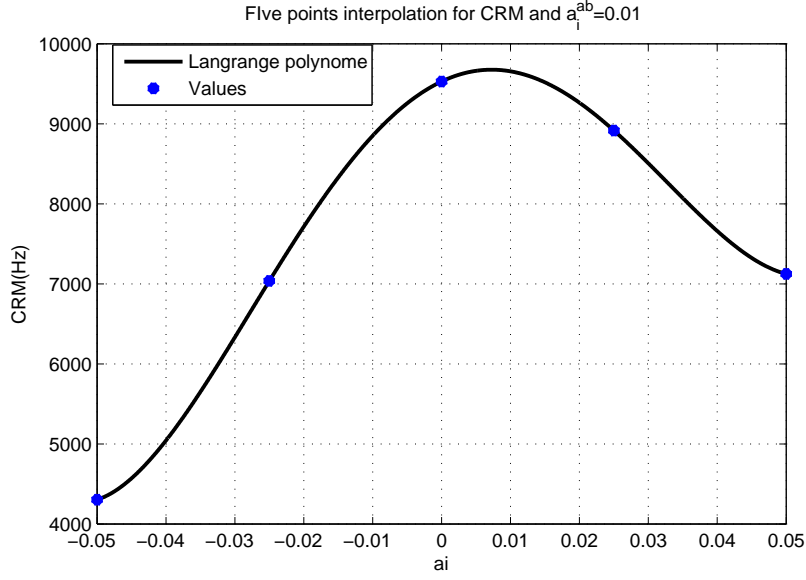


Figure 2.1: Five points measurement interpolation for CRM

2.2 Gradient based methods

After the Non-gradient methods are implemented, for better control results, some gradient based methods like Gauss-Newton algorithm and Levenberg-Marquardt algorithm can be applied for the identification of the aberrations. As all the dominant modes have been optimized to the some point, we can consider that the coupling between the modes is small and the equations modeled for CRM can be taken as the model that can be used for identification of the aberrations.

2.2.1 Gauss-Newton algorithm

Gauss-Newton algorithm is used to solve non-linear least square problems. This method can be used for the identification of the unknown parameters in our estimation that can be presented as:

$$\beta^T = [\overline{CRM}^{opt}, a_1^{ab}, a_2^{ab}, \dots, a_i^{ab}] \quad (2.1)$$

The unknown parameters in this case are the amplitudes for each mode separately and the optimal value of CRM that should be obtained after the optimization. In this case we are going to use the method to minimize the cost function(i.e, the non aberrated CRM value):

$$\min_{\beta} S \quad (2.2)$$

$$S = \sum_{j=1}^m r_j^2 \quad (2.3)$$

where r_j presents the error between the estimated value of CRM and y_j , the measurements obtained from the real system:

$$r_j = y_j - \overline{CRM}_j^{ab}(\overline{CRM}^{opt}, a_1^{ab}, a_2^{ab}, \dots, a_i^{ab}), j = 1, 2, \dots, n \quad (2.4)$$

and the measurement matrix of the measurements y_j , taken at some points x_j , can be presented as:

$$y = \begin{bmatrix} y_1(x_1) \\ y_2(x_2) \\ y_3(x_3) \\ \vdots \\ y_m(x_m) \end{bmatrix} \quad (2.5)$$

To find the optimal solution, the error should be minimized:

$$\frac{\partial S}{\partial \beta_i} = 2 \sum_{j=1}^m r_j \frac{\partial r_j}{\partial \beta_i} = 0 \quad (2.6)$$

If we develop the Equation 2.6 to calculate the unknown parameters in β :

$$J_r^T \cdot J_r \cdot \Delta \beta = J_r^T \cdot r \quad (2.7)$$

$$\beta^{n+1} = \beta^n + (J_r^T \cdot J_r)^{-1} \cdot J_r^T \cdot r \quad (2.8)$$

$$\Delta \beta^T = [\Delta \overline{CRM}^{opt} \Delta a_1^{ab} \Delta a_2^{ab} \dots \Delta a_i^{ab}], \quad (2.9)$$

where, J_r is the Jacobean. Here, the inversion of the matrix $(J_r^T \cdot J_r)$ for small number of measurement points can give problem by inverting with the MATLAB, `inv()` function. For this aim the pseudo-inversion using the SVD-Singular Value Decomposition can be performed. The code is presented on the Fourth Appendix. For this case we have:

$$J_r = \frac{\partial y}{\partial \beta_{x_j}} \quad (2.10)$$

$$J_r = \begin{bmatrix} \frac{\partial \overline{CRM}^{ab}}{\partial \overline{CRM}^{opt}} x_1 & \frac{\partial \overline{CRM}^{ab}}{\partial a_1^{ab}} x_1 & \dots & \frac{\partial \overline{CRM}^{ab}}{\partial a_i^{ab}} x_1 \\ \frac{\partial \overline{CRM}^{ab}}{\partial \overline{CRM}^{opt}} x_2 & \frac{\partial \overline{CRM}^{ab}}{\partial a_1^{ab}} x_2 & \dots & \frac{\partial \overline{CRM}^{ab}}{\partial a_i^{ab}} x_2 \\ \vdots & \vdots & \ddots & \vdots \\ \frac{\partial \overline{CRM}^{ab}}{\partial \overline{CRM}^{opt}} x_m & \frac{\partial \overline{CRM}^{ab}}{\partial a_1^{ab}} x_m & \dots & \frac{\partial \overline{CRM}^{ab}}{\partial a_i^{ab}} x_m \end{bmatrix} \quad (2.11)$$

The derivatives according to the \overline{CRM}^{ab} are calculated as following:

$$\frac{\partial \overline{CRM}^{ab}}{\partial \overline{CRM}^{opt}} = e^{-2(\frac{2\pi\sigma_{wf}}{\lambda})^2} \quad (2.12)$$

$$\frac{\partial \overline{CRM}^{ab}}{\partial a_i^{ab}} = -16 \cdot (a_i^{ab} - a_i^c) \cdot \overline{CRM}^{opt} \cdot \frac{\pi^2}{\lambda^2} \cdot e^{-2(\frac{2\pi\sigma_{wf}}{\lambda})^2} \quad (2.13)$$

2.2.2 Levenberg - Marquardt algorithm

The Levenberg - Marquardt algorithm can be developed from the Gauss Newton algorithm with adding the diagonal element, $J_r^T J_r$, and by adding a dumping factor, μ :

$$\beta^{n+1} = \beta^n + (J_r^T \cdot J_r + \mu \text{diag}(J_r^T J_r))^{-1} \cdot J_r^T \cdot r \quad (2.14)$$

Here the dumping factor μ can be adjusted according to the reduction of S. If the reduction is fast like in our case, we can use small μ , and this method will be similar to the previous Gauss-Newton method. If an iteration gives insufficient reduction in the residual, can be increased, giving a step closer to the gradient descent direction.

2.2.3 Single mode correction

After the most of the dominant modes are corrected by the Non-gradient used methods before and most of the aberrations are corrected, the following assumption can be taken:

$$\sigma_{wf}^2 \approx 0; \text{ leads to : } e^{-2(\frac{2\pi\sigma_{wf}}{\lambda})^2} \approx 1, \quad (2.15)$$

this means, if we want to correct one mode separately we can assume that the following equation is correct:

$$\overline{CRM}^{ab} = \overline{CRM}^{opt} e^{-2(\frac{2\pi}{\lambda})^2 \cdot \sum_{j=1}^m (a_j^{ab} - a_j^c)^2} \approx \overline{CRM}^{opt} e^{-2(\frac{2\pi}{\lambda} (a_i^{ab} - a_i^c))^2} \quad (2.16)$$

Using the Equation. 2.16 we can perform correction on single mode using the following Jacobean:

$$J_r = \begin{bmatrix} \frac{\partial \overline{CRM}^{ab}}{\partial \overline{CRM}^{opt}} x_1 & \frac{\partial \overline{CRM}^{ab}}{\partial a^{ab}} x_1 \\ \frac{\partial \overline{CRM}^{ab}}{\partial \overline{CRM}^{opt}} x_2 & \frac{\partial \overline{CRM}^{ab}}{\partial a^{ab}} x_2 \\ \vdots & \vdots \\ \frac{\partial \overline{CRM}^{ab}}{\partial \overline{CRM}^{opt}} x_m & \frac{\partial \overline{CRM}^{ab}}{\partial a^{ab}} x_m \end{bmatrix} \quad (2.17)$$

Using this assumptions, we can do identification of the aberration on each Zernike mode separately.

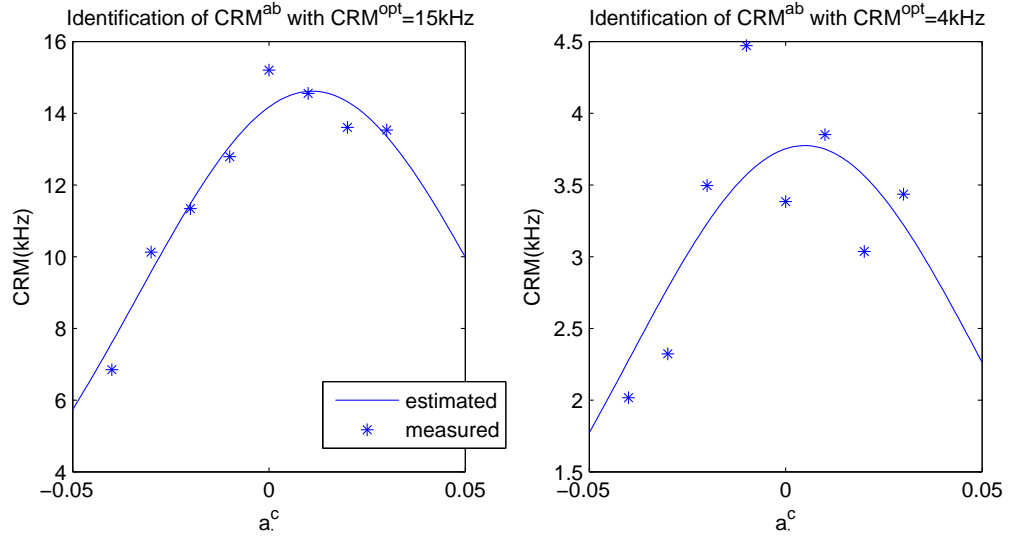


Figure 2.2: Identification of the CRM^{ab} on the simulated data for the mode a_{13} , for high $CRM^{opt} = 15kHz$ and more noisy $CRM^{opt} = 4kHz$ and the aberration $a_{13}^{ab} = 0.01\mu m$

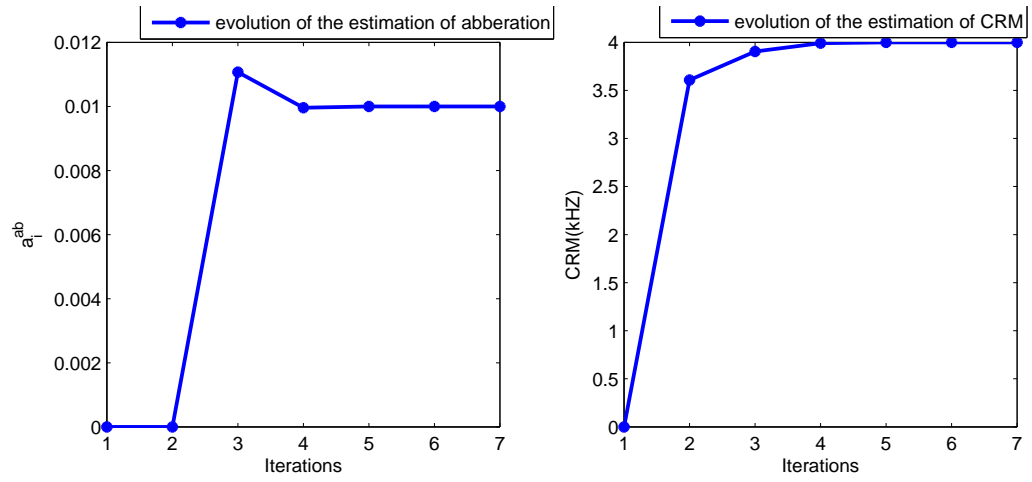


Figure 2.3: Evolution of the identification of the parameters CRM=4kHz and $a_i^{ab} = 0.01\mu m$ with Levenberg - Marquardt method

Chapter 3

Implementation and results

3.1 Non-gradient based methods implementation results

3.1.1 Results from the testing on the real system

When the code is implemented on the real system, the two parameters: *acceleration* and the initial *Step size* should be adjusted according to the specific nature of the system in order to get the best accuracy and good convergence. The Hill-climbing method is presented in Chapter 2 and the pseudo-code is presented in the Second Chapter. For this aim, two cases were tested on the real system. In the first case, *acceleration* = 1.2 and the initial *Stepsize* = 0.015 has been taken and on the second experiment, *acceleration* = 1.5 and the initial *Step size* = 0.05.

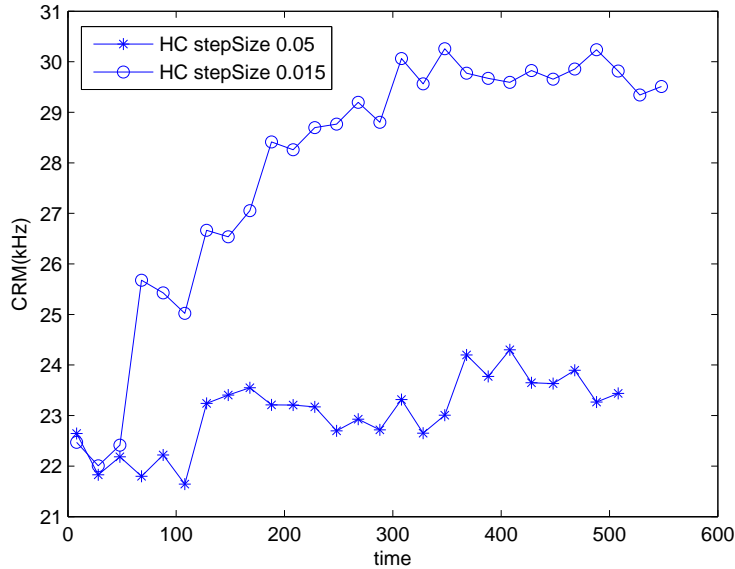


Figure 3.1: Hill-climbing method for different Step sizes

The test results are presented in Fig. 3.1. After the running of the two algorithms with

different parameters, we can see that the plots for the two cases presented in one graph. From the plot, we can easily conclude that the smaller step size will present better optimization and that the bigger steps size found difficulty to determine the optimal points and presented more oscillation during the optimization. According to this for the future examination we are going to use the *acceleration* = 1.2 and *Step size* = 0.015 for the optimization with the Hill-Climbing method.

3.2 3N-algorithm for optimization

The 3N-algorithm is based on the interpolation of the CRM for single mode, using interpolation with measurement in three points. After the three measurements are taken, the maximum of the interpolating function is calculated and the point with the highest value of the interpolated metric is taken for optimal point.

In our case, because of the our previous knowledge about the interval where most probably the amplitudes of the aberrations, we are taking three measurements for every aberration for ± 0.05 and 0. If the aberration is out of this boundaries we shift the measurement for the next iteration to higher or lower interval according to the value of the amplitude of the aberration.

3.2.1 Comparison of the two algorithms

After we implemented the 3N algorithm and the Hill-climbing algorithm, we are going to do some comparison between the two methods for optimization. The two algorithms were performed on the same measurement and were performed two iteration cycles for all the concerning modes. The order of execution of the optimization for the modes was following: $a_{13}, a_{25}, a_{13}, a_{25}, a_4, a_6, a_8, a_9$ and the results of the optimization performed on the real system are presented on Fig.3.2

For the first comparison we used measurement in 4 second and high intensity to the laser light. When we see the plots for the outposts of the two methods, we can notice that the 3N method is faster than the HC method, this is due to the fact that this algorithm uses 3 measurements comparing to the 5 measurements that HC method uses for one iteration. On the other hand, we can notice that in this case the HC algorithm will reach higher value for measurement of CRM, that means that the optimization is more effective with this method but slower.

Comparison of the two algorithms with higher noise measurements

Because when the experiment is performed on the real biological material, the intensity of the light of the laser is decreased in order to prevent the biological material from damaging with high laser intensity. This means that in this case we are going to have smaller number of measured photon per one measurement cycle, so the noise level will increase and the accuracy of the measurement will decrease. The aim of this experiment is to compare the two algorithms when they are performed during the examination of tissues. In this comparison were performed two cycles iterations with the two methods and one measurement was performed on time duration of four seconds.

According to the results presented on Fig. 3.3 , the 3-N algorithm proved to be more robust than HC for the increased measurement noise during this measurements.

3.2.2 Multivariable interpolation results

The multivariable interpolation was performed on the coupled modes a_{13} and a_{25} and on the Fig. 3.4 is presented the comparison of the theoretical distribution of CRM and the

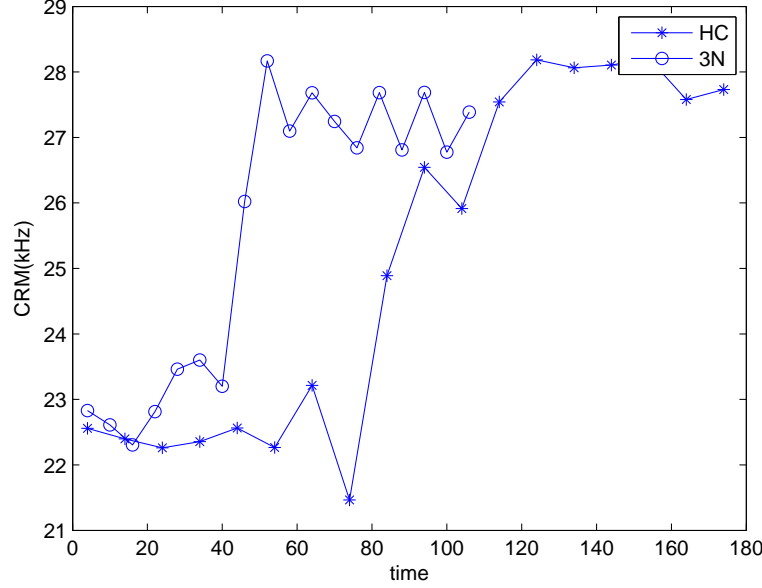


Figure 3.2: Comparison of the two methods

measured interpolated plot. The time for one measurement was taken to be 4s and other modes were previously corrected. We can notice that if the other dominant modes are corrected, the coupling between these two modes is small, that it can be neglected. This means that if the aberration is corrected for the most dominant modes, the aberrations for single mode can be presented with the equation 2.16.

3.3 Gradient based method implementation

After the Non-gradient methods were performed for the optimization on the deformable mirror, the optimization result obtained with this optimization method can be used like a basis for implementation of the model based methods for the optimization.

After the correction performed using the non-gradient based methods, most of the aberrations are corrected and the coupling between the modes is low. This means that we can use the theoretical model for the estimation of CRM depending on the aberration level for improving the estimation of the amplitudes of the Zernike modes.

For the testing of the gradient-based methods we used the created computer simulation generated data that simulates the estimation of CRM . With adding noise to the simulation data we are going to replicate the noisy environment during measurement. The main aim of using the simulation data is for the testing the efficiency and the accuracy of the optimization methods.

3.4 Levenberg- Marquardt algorithm

The first method that was implemented was the NLLS method that was explained on the previous chapter. This means that for the optimization method in this case, the Hessian will be provided to the optimization method by using the exact Jacobean calculated directly from the equation expressing the CRM . The testing was performed after

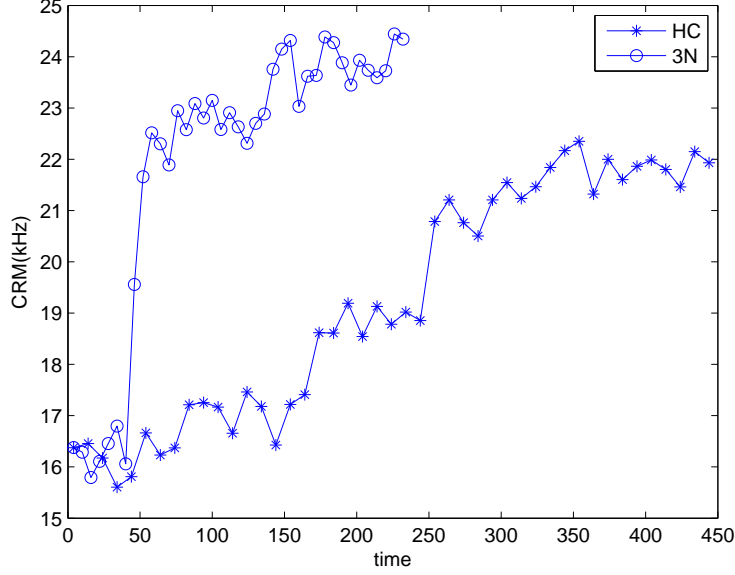


Figure 3.3: Comparison of the two methods with more measurement noise

measurement points were obtained by setting different values for a_c for separate Zernike modes. The algorithm was tested for different values of the molecular brightness and for the number of measurement points. For every evaluation point the measurement experiment was performed 50 times. To compare the performance of each method, the Root Mean Square of the errors, and also the Maximal Absolute Value of estimated error for the measurement with highest noise is presented in order to test the methods for different measurements and their robustness to the different measurement noise. The plots are presented on Fig. 3.5.

As we can see from the results presented on Fig. 3.5, the efficiency of the optimization with this method highly depends from the level of the molecular brightness, CRM.

3.5 Optimization with fminunc and fminsearch

Because the acquisition card NI PCIe-6321 that is used in the system for generating the data is compatible with MATLAB Data Acquisition Toolbox, we can use the functions that are provided for nonlinear unconstrained optimization techniques in MATLAB. For this aim the two functions fminunc (Medium scale algorithm) and fminsearch can be used for optimization.

The fminunc function for medium scale optimization uses the BFGS Quasi-Newton method with a mixed quadratic and cubic line search procedure and fminsearch uses the simplex search method that does not use numerical or analytic gradients

For the optimization, we tested the data with several cost functions:

$$(Norm\ 1)\ S_1(\beta) = \sum_{k=1}^N (CRM_k^{mes} - \overline{CRM}_k^{ab}(\beta))^2 \quad (3.1)$$

$$(Norm\ 2)\ S_2(\beta) = \sum_{k=1}^N \left| CRM_k^{mes} - \overline{CRM}_k^{ab}(\beta) \right| \quad (3.2)$$

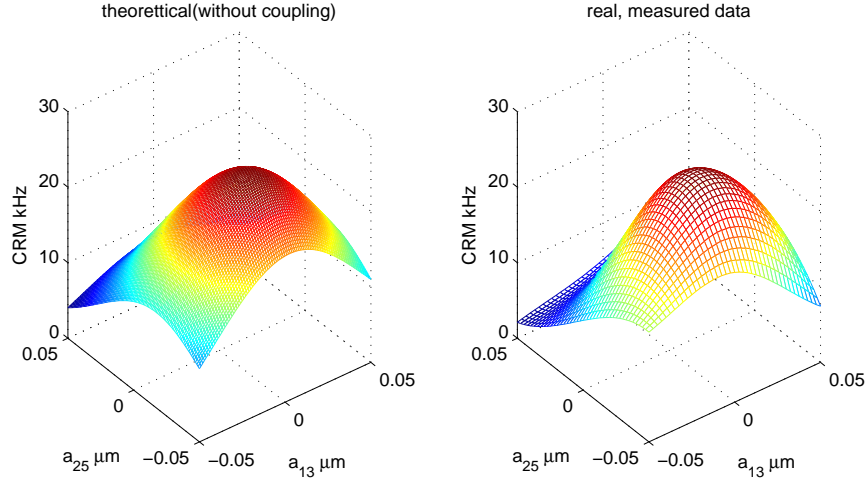


Figure 3.4: Multivariable interpolation of the coupling modes a_{13} and a_{25} , theoretical and measured

$$(Norm\ 3) S_3(\beta) = \max_k \left| CRM_k^{mes} - \overline{CRM}_k^{ab}(\beta) \right| \quad (3.3)$$

All of this cost function was tested with the different methods for optimization in order to compare the different optimization method performances. For each test, the same starting point was taken to compare the final values for the aberration obtained after the optimization. Each method performed on different cost functions was evaluated according to the accuracy of the identification of the generated aberration and the numbers of iterations that are required for finding the solution. The algorithms were tested for simulation data with presented aberration on single mode $a_i^c = 0.01\mu m$ and for different values of $CRM = 4kHz$ and $CRM = 15kHz$. The testing was performed for different number of measurement points and one measurement was taken to be 4 seconds. To compare the performance of each method, the Root Mean Square of the errors, and also the Maximal Absolute Value of estimated error for the measurement with highest noise is presented. The testings for each point were repeated 50 times.

As it is expected, if we compare the plots from the testing with Levenberg-Marquardt method Fig.3.5 and the plots presented with the comparison of the `fminunc` and `fminsearch` on Fig.3.7 and 3.6, the results obtained with the Levenberg-Marquardt method have best performance. The main reason for this results is due to the fact that the Hessian was provided by using the exact formula for CRM and the other methods are using numerical approach to obtain the gradient. Also, we can see that the both optimization functions `fminunc` and `fminsearch` are giving good optimization results using the Norm 1 for the optimization. The optimization performance is lower if the CRM is small, because of higher measurement noise impact in this case. The `fminunc` optimization for Norm 2 and Norm 3 was not effective and didn't find the optimal solution for low level of CRM, and the results are not presented on the plots presented in 3.7.

If we compare the speed of iterations needed for the optimization methods, the Levenberg-Marquardt method also gives superior results. In the testing presented on the previous chapter the Levenberg-Marquardt, was able to reach the optimal solution with only 4-15 iterations. On the other hand, the `fminunc` needed about 10-20 iterations when it was performed on the higher CRM data and `fminsearch` needed about 48-90 iterations for the optimization. When the optimization was performed on the higher measurement data the number of iterations with `fminunc` and `fminsearch` sometimes exceeded over 200

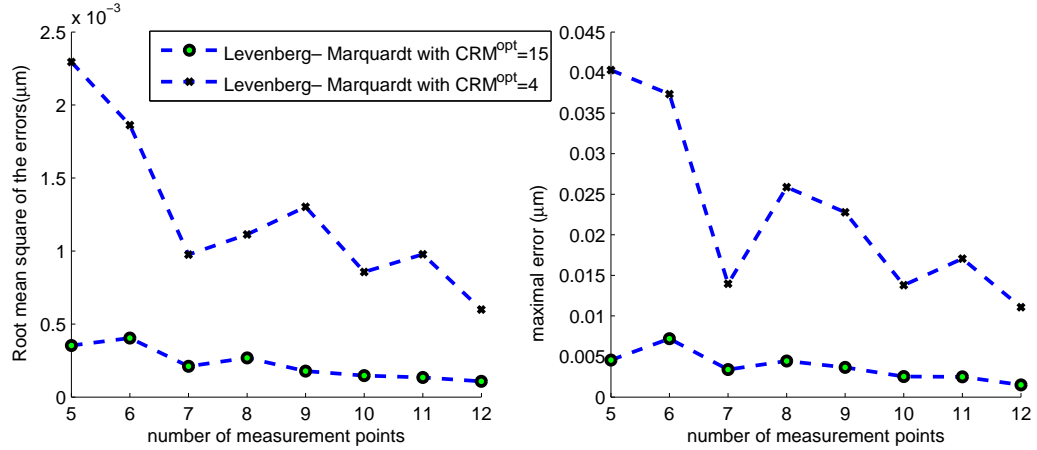


Figure 3.5: Levenberg- Marquardt algorithm optimization results for different number of measurement points for $CRM=15\text{kHz}$ and $CRM=4\text{kHz}$ and aberration $a_{13}^{ab} = 0.01\mu\text{m}$

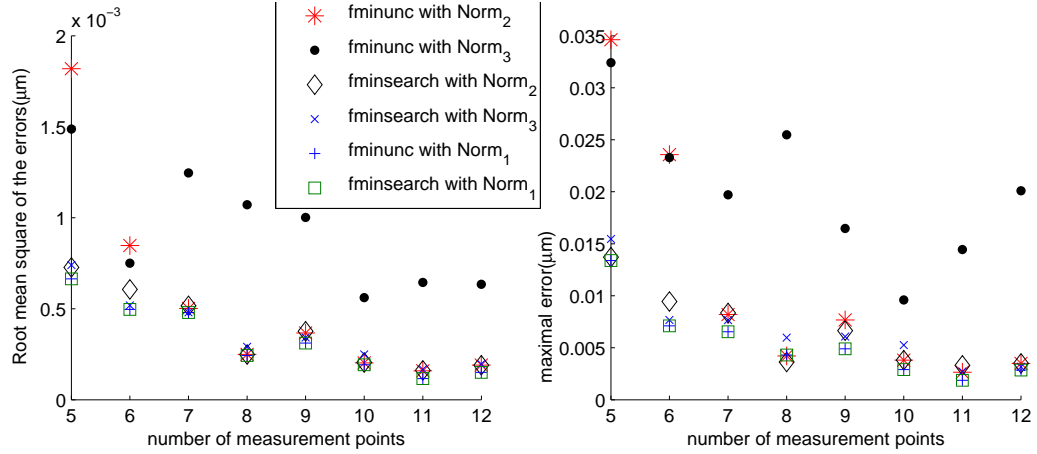


Figure 3.6: Optimization results for estimating the aberration with $CRM^{opt} = 15\text{kHz}$ and 4 seconds measurements

iterations for this two methods, that was the limit number given to the solver.

3.6 Implementation of the model-based methods on the real systems data

After the testing of all of the methods for the different cost functions, the real data measurements were obtained from the system and the code was tested on this data. Two kind of measurement data were obtained:

- High precision data taken with long measurement
- Low precision data taken with short 4s measurements around the optimization point

In this case the testing of the results with 4 seconds measurement taken around the optimization point that was found before using the non-gradient methods was performed

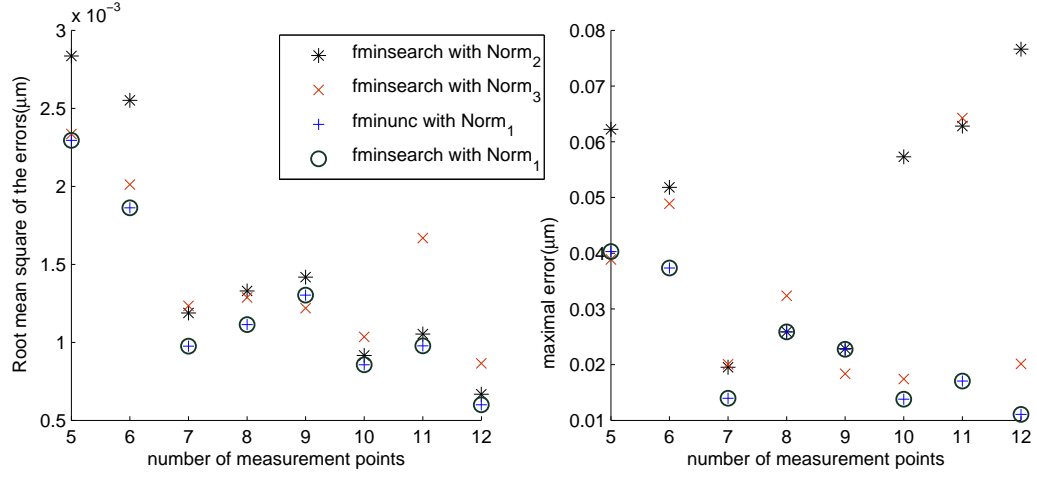


Figure 3.7: Optimization results for estimating the aberration with $CRM^{opt} = 4kHz$ and 4 seconds measurements

to simulate the online algorithm of gradient based method. The short time measurements have more measurement noise than the theoretical ones.

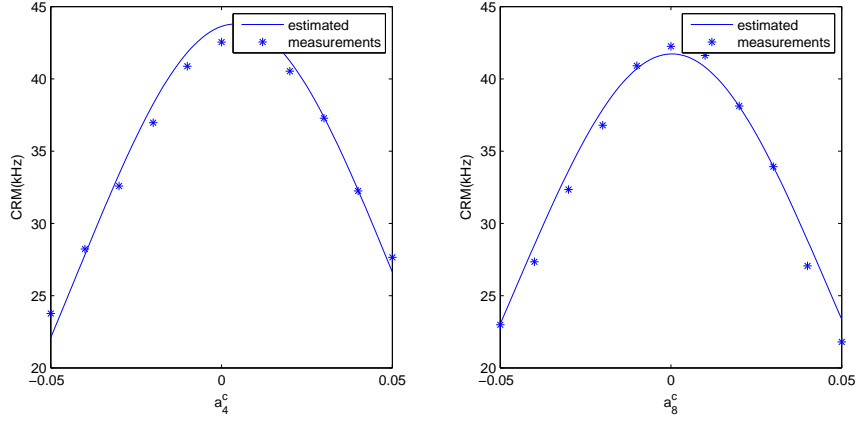


Figure 3.8: Implementation of the Levenberg-Marquardt method on measurements taken from the real system performed on longer measurement time, with low noise level for the modes a_4 and a_8

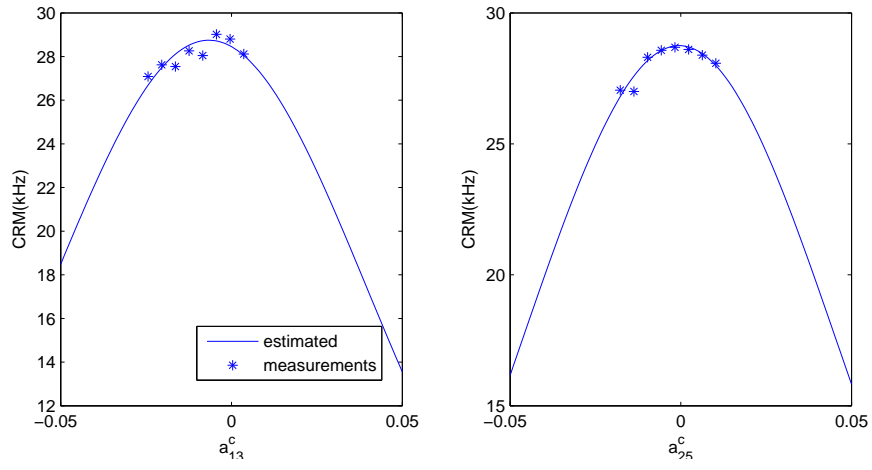


Figure 3.9: Implementation of the Levenberg-Marquardtmethod on measurements taken from the real system performed on 4 seconds measurement time, with higher noise level for the modes a_{13} and a_{25}

Chapter 4

Conclusions and future improvements

In this work was presented the aberration correction using the measured molecular brightness, CRM. The relation between CRM and the aberrations in the measurements can be good estimated with exact mathematical expression 1.1, especially for low amplitude of the aberrations. The model-based methods proved to be effective for the optimization and robust to the high measurement noise especially for simulations where the molecular brightness was small. Despite of the good model of CRM, the measurement time for the estimation of the aberrations is very high. Because in reality the experiments are performed on real biological materials and the optimization should be performed as fast as possible. This means that some new approach should be experimented. After providing the new model for the number of molecules presented with Equation.1.5, the Count Rate, CR can be well evaluated theoretically by its relation with CRM and N. The Count Rate has also convex shape and reaches it maximum as the aberrations are corrected. The CR is proportional with the number of measured photons. This means that the evaluation of the measured value of CR can be estimated with shorter period of measurement. In this case, for the optimization some non-gradient optimization methods can be performed, similar like using the CRM but with significant faster optimization time. This can leads to faster optimization and possible implementation of new, more complex optimization methods.

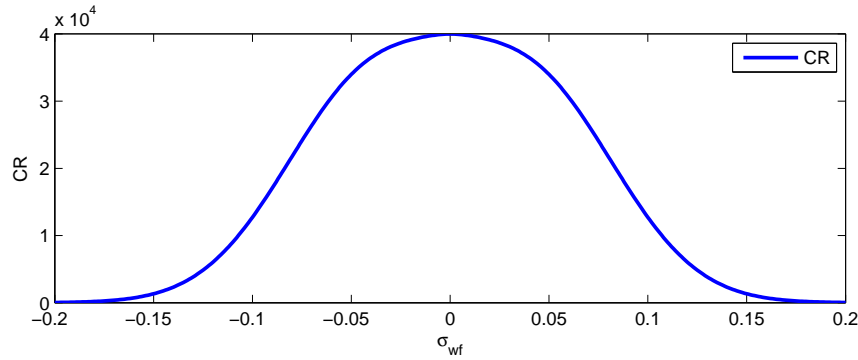


Figure 4.1: Representation of CR for a_{13} with $CRM = 4kHz$ and $N=4$

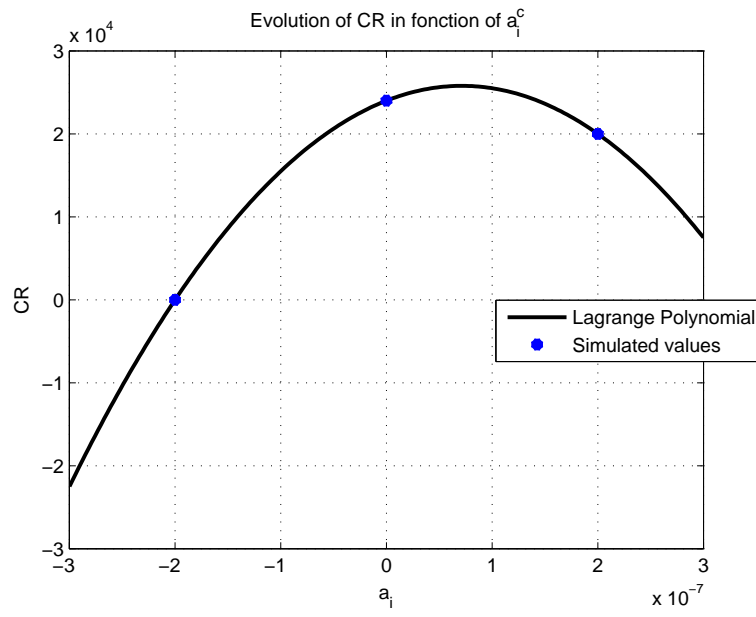


Figure 4.2: Optimization of CR using lagrangian interpolation for a_{13}^c with 3 point measurements, CRM=4kHz and N=10 and measurement time 0.1s and $a_{13}^{ab} = 0.1\mu m$

Bibliography

- [1] TUDOR-BOGDAN AIRIMITOAI, *Rapport de travail sur l'optique adaptive*, GIPSA-lab, Novembre 2012
- [2] C.E.LEROUX, I.WANG, J.DEROUARD, A.DELON, *Adaptive Optics for Fluorescence Correlation Spectroscopy*, Optical Society of America, 2011
- [3] H.SONG, *Model-Based control in adaptive optics systems*, Ph.D. dissertation, Delft University of Technology, 2011
- [4] Y.LIU, J.MA, B.LI, Y.HU, J.CHU, *Comparaison of optimization algorithms for adaptive optics system without a wavefront sensor*, 6th International Symposium on Advanced Optical Manufacturing and Testing Technologies: Large Mirrors and Telescopes, 2012
- [5] Y.LIU, J.MA, B.LI, Y.HU, J.CHU, *Hill-climbing algorithm based on Zernike modes for wavefront sensorless adaptive optics*, Optical Engineering, 2013
- [6] M.J.BOOTH, *Wave front sensor-less adaptive optics: a model-based approach using sphere packings*, Optics Express, 2006
- [7] Z.MICHALEWICZ, DAVID B.FOGEL, *How to solve it: Modern Heuristics*, Springer, 2000
- [8] MICHAELLE A.DIGMAN, E. GRATTON *Lessons in Fluctuation Correlation Spectroscopy*, Annu. Rev. Phys. Chem., 2011
- [9] J.H.MATHEWS, K.D.FINK *Numerical Methods Using MATLAB*, Prentice Hall, 1999
- [10] Q.N.TRAN, E.WITRANT, N.BORDET *Optimisation parametrique d'un modele de moteur diesel a injections multiples*, IEEE Conf. Int. Francophone dAutomatique (CIFA) , Grenoble, France, 2012
- [11] M.S.BAZARAA, H.D.SHERALI, C.M.SHETTY *Nonlinear Programming, Theory and algorithms* John Wiley & Sons, Inc., 2006
- [12] M.BORN, E.WOLF *Principles of Optics*, Cambridge University Press, 6th ed. 1980

Chapter 5

The First Appendix, Zernike polynomials

In mathematics, the Zernike polynomials are a sequence of polynomials that are orthogonal on the unit disk. These polynomials are a complete set in two variables, r and Θ , that are orthogonal in a continuous fashion over the unit circle. θ is the azimuthal angle, and r is the radial distance. The first few Zernike modes ordered by Noll index are presented on Tab.5.1 and two-dimensional representation of the first Zernike Modes on Fig.5.1

i	n	m	$Z_i(r, \theta)$	Aberration term
1	0	0	1	Piston
2	1	1	$2r\cos(\theta)$	Tip
3	1	-1	$2r\sin(\theta)$	Tilt
4	2	0	$\sqrt{3}(2r^2 - 1)$	Defocus
5	2	2	$2\sqrt{3}r^2\cos(2\theta)$	Astigmatism
6	2	-2	$2\sqrt{3}r^2\sin(2\theta)$	Astigmatism
7	3	1	$2\sqrt{2}(3r^3 - 2r)\cos(\theta)$	Coma
8	3	-1	$2\sqrt{2}(3r^3 - 2r)\sin(\theta)$	Coma
9	3	3	$2\sqrt{2}r^3\cos(3\theta)$	
10	3	-3	$2\sqrt{2}r^3\sin(3\theta)$	
11	4	0	$\sqrt{5}(6r^4 - 6r^2 + 1)$	Spherical (1st)
12	4	2	$\sqrt{10}(4r^4 - 3r^2)\cos(2\theta)$	
13	4	-2	$\sqrt{10}(4r^4 - 3r^2)\sin(2\theta)$	
14	4	4	$\sqrt{10}r^4\cos(4\theta)$	
15	4	-4	$\sqrt{10}r^4\sin(4\theta)$	
16	5	1	$2\sqrt{3}(10r^5 - 12r^3 + 3r)\cos(\theta)$	
17	5	-1	$2\sqrt{3}(10r^5 - 12r^3 + 3r)\sin(\theta)$	
18	5	3	$2\sqrt{3}(5r^5 - 4r^3)\cos(3\theta)$	
19	5	-3	$2\sqrt{3}(5r^5 - 4r^3)\sin(3\theta)$	
20	5	5	$2\sqrt{3}r^5\cos(5\theta)$	
21	5	-5	$2\sqrt{3}r^5\sin(5\theta)$	
22	6	0	$\sqrt{7}(20r^6 - 30r^4 + 12r^2 - 1)$	Spherical (2nd)

Table 5.1: The first few Zernike modes ordered by Noll index

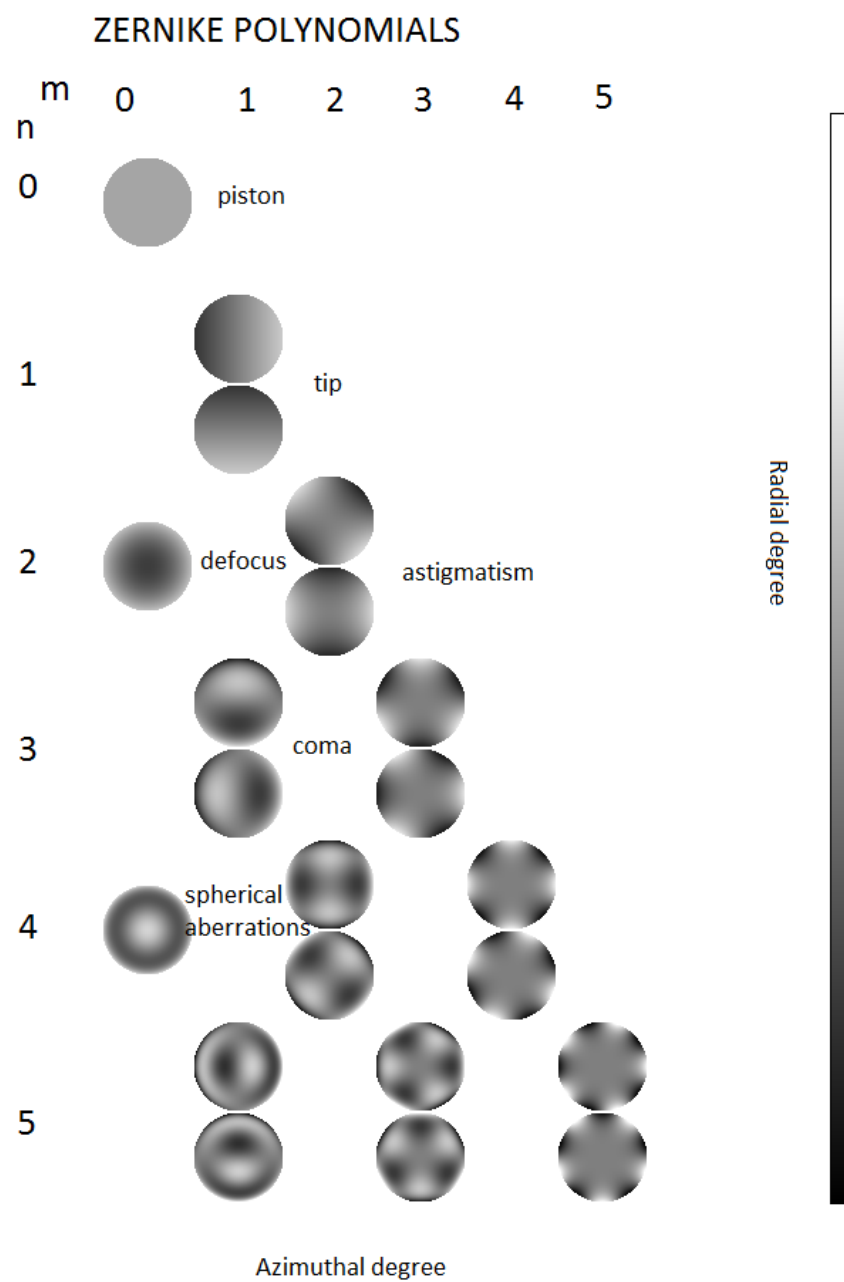


Figure 5.1: two-dimensional representation of the first Zernike Modes

Chapter 6

The Second Appendix, Pseudocode for the HC algorithm

The algorithm used for the implementing the HC algorithm was programmed for Continuous Space Hill Climbing Algorithm problem. The pseudocode is given like following:

```
stepSize = initialStepSizes; // a vector of all 1's is common
acceleration = someAcceleration; // a value such as 1.2 is common
candidate[0] = -acceleration;
candidate[1] = -1 / acceleration;
candidate[2] = 0;
candidate[3] = 1 / acceleration;
candidate[4] = acceleration;
while (EVAL(currentPoint) - before) < epsilon do
    for each element i in currentPoint do
        best = -1;
        bestScore = -INF;
        for j from 0 to 4 do
            currentPoint[i] = currentPoint[i] + stepSize[i] * candidate[j];
            temp = EVAL(currentPoint);
            currentPoint[i] = currentPoint[i] - stepSize[i] * candidate[j];
            if temp > bestScore then
                bestScore = temp;
                best = j;
            end
            if candidate[best] is not 0 then
                currentPoint[i] = currentPoint[i] + stepSize[i] * candidate[best];
                stepSize[i] = stepSize[i] * candidate[best]; // accelerate
            end
        end
    end
end
```

Algorithm 1: The pseudocode for the Hill-climbing algorithm

Chapter 7

The Third Appendix, Estimation of N

$$\hat{N} = \frac{\bar{n}^2}{n(t)n(t + \delta t) - \bar{n}^2} \quad (1) \quad (7.1)$$

$$\hat{N} = \frac{\bar{n}^2}{var(n) - \bar{n}} \quad (2) \quad (7.2)$$

CRM real	N real	N estimated with (1)	N estimated with (2)
10	5	2.0284	3.8402
20	5	3.2333	4.2377
30	5	3.8081	4.3009
1	50	3.3314	13.7979
3	50	15.4128	30.2752
5	50	51.9205	36.4039
10	50	-64.4876	43.6743
1	150	16.3551	51.2684
2	150	-282.1378	85.1997
3	150	-35.6562	112.8373
4	150	-29.1586	124.0409

Table 7.1: Estimation of N with Eq.1 and 2

Chapter 8

The Fourt Appendix, Inversion with SVD

Code for pseudo-inversion in MATLAB using singular value decomposition. Matrix of a matrix $A(m \times n)$, use `svd()`,... $A=U*S*V$:

```
[m,n] = size(A);  
[U, S, V] = svd(A);  
r = rank(S);  
SR = S(1:r, 1:r);  
SRc = [SR-1 zeros(r, m-r); zeros(n-r, r) zeros(n-r, m-r)];  
Apseu = V * SRc * U.;
```